

SANDIA REPORT

SAND2005-1718
Unlimited Release
Printed March 2005

Glider Communications and Controls for the Sea Sentry Mission

Jeffrey L. Dohner and John T. Feddema

Prepared by
Sandia National Laboratories
Albuquerque, New Mexico 87185 and Livermore, California 94550

Sandia is a multiprogram laboratory operated by Sandia Corporation,
a Lockheed Martin Company, for the United States Department of Energy's
National Nuclear Security Administration under Contract DE-AC04 94AL85000.

Approved for public release, further dissemination unlimited.



Sandia National Laboratories

Issued by Sandia National Laboratories, operated for the United States Department of Energy by Sandia Corporation.

NOTICE: This report was prepared as an account of work sponsored by an agency of the United States Government. Neither the United States Government, nor any agency thereof, nor any of their employees, nor any of their contractors, subcontractors, or their employees, make any warranty, express or implied, or assume any legal liability or responsibility for the accuracy, completeness, or usefulness of any information, apparatus, product, or process disclosed, or represent that its use would not infringe privately owned rights. Reference herein to any specific commercial product, process, or service by trade name, trademark, manufacturer, or otherwise, does not necessarily constitute or imply its endorsement, recommendation, or favoring by the United States Government, any agency thereof, or any of their contractors or subcontractors. The views and opinions expressed herein do not necessarily state or reflect those of the United States Government, any agency thereof, or any of their contractors.

Printed in the United States of America. This report has been reproduced directly from the best available copy.

Available to DOE and DOE contractors from
U.S. Department of Energy
Office of Scientific and Technical Information
P.O. Box 62
Oak Ridge, TN 37831

Telephone: (865)576-8401
Facsimile: (865)576-5728
E-Mail: reports@adonis.osti.gov
Online ordering: <http://www.osti.gov/bridge>

Available to the public from
U.S. Department of Commerce
National Technical Information Service
5285 Port Royal Rd
Springfield, VA 22161

Telephone: (800)553-6847
Facsimile: (703)605-6900
E-Mail: orders@ntis.fedworld.gov
Online order: <http://www.ntis.gov/help/ordermethods.asp?loc=7-4-0#online>



SAND2005-1718
Unlimited Release
Printed March 2005

Glider Communications and Controls for the Sea Sentry Mission

Jeffrey L. Dohner
Integrated Microsystems
jldohne@sandia.gov

John T. Feddema
Intelligent Systems Controls
jtfedde@sandia.gov

Sandia National Laboratories
P.O. Box 5800
Albuquerque, NM 87185

ABSTRACT

This report describes a system level study on the use of a swarm of sea gliders to detect, confirm and kill littoral submarine threats. The report begins with a description of the problem and derives the probability of detecting a constant speed threat without networking. It was concluded that glider motion does little to improve this probability unless the speed of a glider is greater than the speed of the threat. Therefore, before detection, the optimal character for a swarm of gliders is simply to lie in wait for the detection of a threat. The report proceeds by describing the effect of noise on the localization of a threat once initial detection is achieved. This noise is estimated as a function of threat location relative to the glider and is temporally reduced through the use of an information or Kalman filtering. In the next section, the swarm probability of confirming and killing a threat is formulated. Results are compared to a collection of stationary sensors. These results show that once a glider has the ability to move faster than the threat, the performance of the swarm is equal to the performance of a stationary swarm of gliders with confirmation and kill ranges equal to detection range. Moreover, at glider speeds greater than the speed of the threat, swarm performance becomes a weak function of speed. At these speeds swarm performance is dominated by detection range. Therefore, to future enhance swarm performance or to reduce the number of gliders required for a given performance, detection range must be increased. Communications latency is also examined. It was found that relatively large communication delays did little to change swarm performance. Thus gliders may come to the surface and use SATCOMS to effectively communicate in this application.

This report summarizes work completed for DARPA under Proposal Number 062030407-2 funded by MIPR 04-Q104 and Sandia National Laboratories (SNL) contract DE-AC04-94AL85000.

Intentionally Left Blank

ACKNOWLEDGEMENTS

We would like to thank Khine Latt, the DARPA Program Manager for this project, for the opportunity to work on this challenging problem and for her technical guidance and support throughout the project. We would also like to thank Samuel Earp and Edward Mihalak for their technical and programmatic suggestions, and Robert Miyamoto, James Luby, and Michael Boyd of the University of Washington for their assistance on the range of acoustic transmission and glider control.

Intentionally Left Blank

TABLE OF CONTENT

I. INTRODUCTION	12
II. DETECTION	14
III. LOCALIZATION	15
<i>a Measurement noise</i>	16
<i>b Information filtering</i>	19
IV. CONFIRMATION AND KILL	21
<i>a A higher level of control</i>	21
<i>b A lower level of control</i>	23
<i>c Swarm performance</i>	24
V. CONCLUSIONS	32
VI. FUTURE WORK	33
APPENDIX I: DETECTION RANGE CALCULATION	35
APPENDIX II: SIMULATION PARAMETERS	41
APPENDIX III: LATENCY OF COMMUNICATIONS	43

Intentionally Left Blank

FIGURES:

Figure 1: A swarm of sea gliders are used to detect, localize and kill a threat.....	13
Figure 2: The probability of at least one detection by a swarm of gliders with various glider speeds. Notice that there is little change in the probability of detection with speed.....	15
Figure 3: A glider and its hydrophones. Acoustic energy from a threat reaches the hydrophones at different times. The difference in these arrival times can be used to determine range and bearing.....	16
Figure 4: Time delays between hydrophones are measured using a cross correlation.....	18
Figure 5. Range and bearing error can be translated into a local error in a coordinate system centered at the location of the threat. This error can be translated into global coordinates.....	18
Figure 6: Measurement and prediction of the x location of threat. black – measurement, grey – estimate.....	20
Figure 7: Upper layer of control based on a set of logic rules.....	22
Figure 8: Region of approach to confirm and region of approach to kill.....	23
Figure 9: (a) Configuration used to run Monte Carlo simulations. (b) Results from Monte Carlo simulations. .	24
Figure 10: (a) Configuration used to run Monte Carlo simulation. (b) Probability of a kill. (c) probability of a confirmation.....	26
Figure 11: The region of approach is a function of confirmation and/or detection range and communication latency.....	27
Figure 12: The probability of confirming a threat.....	29
Figure 13: The probability of killing a threat.....	30
Figure 14: The variation in the probability of killing a threat as a function of communication delay. The glider has a speed of 1.5 knots.....	30
Figure 15: As the width of sea space is reduced, the affect of communication delay becomes more significant.....	31
Figure 16: The probability of detecting, confirming and killing a threat as a function of range and number of gliders when the gliders can move faster than the threat.....	29
Figure 17: Wenz’s illustration of back ground noise in the oceans: For frequencies above 1 kHz, noise level are low and are dominated by surface wind speed.....	36
Figure 18: Urick’s combination of data from Wenz, Piggot, and Knudsen: The red line shows the equation (49) approximation to NL for sea state 4 between 1 to 10 kHz.....	36
Figure 19: Spectrum of a WWII fleet boat running a periscope depth: The red line is the equation (50) approximation.....	37
Figure 20: Detection Threshold as a function of frequency for various ranges from the threat:.....	38
Figure 21: Receiver Operating Characteristics (ROC) for Gaussian noise.....	39
Figure 22: Communication range between gliders for a network of gliders using over the surface RF transmission.....	44

Intentionally Left Blank

TABLES:

Table 1: Near- Field anomaly coefficients.....37
Table 2: Attenuation factors.....38
Table 3: Latency of communication45

Intentionally Left Blank

I. INTRODUCTION

In this paper, we present a system level study on the use of swarms of gliders collectively interacting to detect, confirm and kill a littoral submarine threat. Detection implies the initial determination of a possible threat in a sea space, called a contact. Once a contact occurs, localization is used to estimate the position of that contact. This information is communicated to other gliders to determine whether they can confirm and/or whether they are in a position to kill. Confirmation implies that a glider can move close enough to the contact to determine its character through the use of short range sensors, and killing implies being able to physically intercept the threat. In this report, we assumed that contact occurs at an acoustic range of 200 meters (see Appendix I for analysis), confirmation occur at 30 meters, and kill occurs at 5 meters.

A generalized scenario is shown in Figure 1. A lone threat, moving at speed u , enters a rectangular sea space L long and L wide. Within this sea space there is a swarm of N gliders where the i^{th} glider has bearing β_{g_i} and maximum speed v . All gliders have a detection range of $R = 200$ meters. Each glider detects the threat through a set of on-board hydrophones, obeys the same local control law, and is capable of sharing information with neighboring gliders. This study only investigates this two dimensional problem and ignores ocean depth. Assuming that the depth of the ocean is less than the 200 meter detection range, this assumption will not affect the detection analysis; however, it will affect the confirmation and kill analysis and future work is needed in this area.

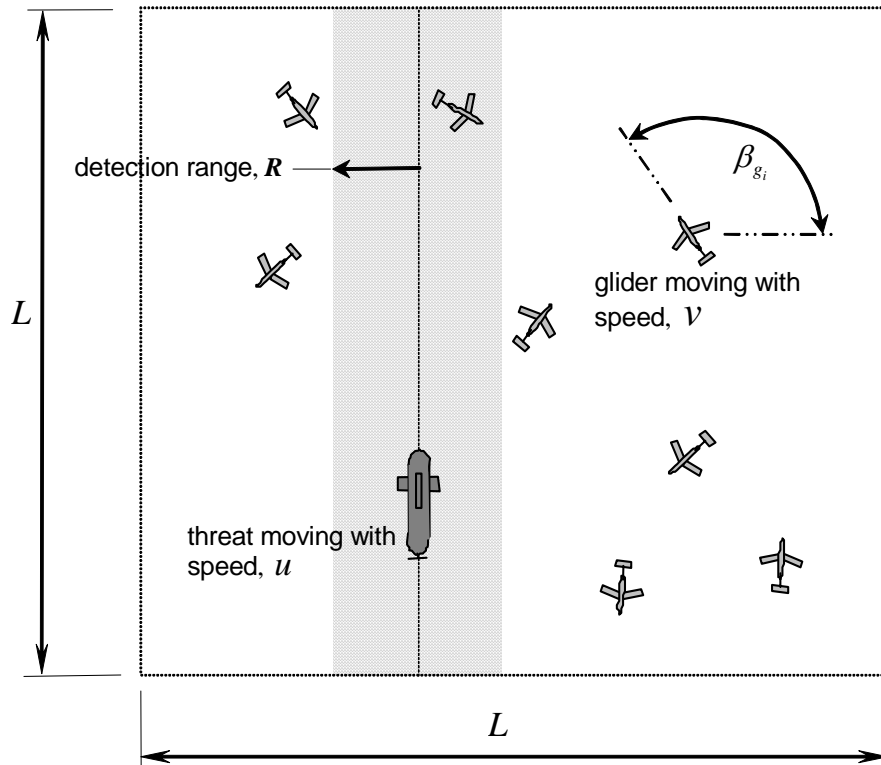


Figure 1: A swarm of sea gliders are used to detect, localize and kill a threat.

II. DETECTION

Detection is the process of determining if a contact is within the Figure 1 sea space. The probability of the swarm detecting this threat, $P_N(S_d)$, is derived from the probability of detection for one glider, $P_{g1}(S_d)$ where

$$S_d = \{\text{detection of threat}\}.$$

We assume that $L = 50$ nm and $u = 3$ knots. Then the detection area $A=2500$ nm² and the time for a threat to cross A is $T = L/u \approx 16.7$ hours. Using the above relations and expanding upon the work of Koopman [1]

$$P_{g1}(S_d) = \frac{4R_{eff}T}{A\pi}(u+v)E(\sigma) \quad (1)$$

where v is the speed of the glider, $E(\sigma)$ is an elliptic integral of the second kind, $\sin \sigma = \frac{2\sqrt{uv}}{u+v}$, and R_{eff} is an effective radius used to account for the sensor integration time, T_{int} , that the threat must be within the detection radius, R , before a contact can be declared. From the work of Wettergren [3], the effective radius for a stationary glider is

$$R_{eff} = \sqrt{R^2 - (uT_{int}/2)^2}. \quad (2)$$

If there are n gliders and if each behaves independently, then the probability of k gliders within the swarm detecting the threat is given by

$$P_N(S_d = k) = \frac{n!}{k!(n-k)!} P_{g1}(S_d)^k (1 - P_{g1}(S_d))^{n-k} \quad (3)$$

and the probability of greater than k detections is given by

$$P_N(S_d > k) = (1 - \sum_{m=0}^k P_N(S_d = m)). \quad (4)$$

Figure 2 is a plot of equation (4) for $k=0$ (at least one detection), $T_{int} = 25$ seconds, $v=0$ knots, $v=0.5$ knots, $v=1.5$ knots, and $v=3.0$ knots. Notice, as stated by Earp [4], motion does little to improve the probability of detection for a glider moving slower than or close to the speed of the threat.

This is an important conclusion. If motion does little to improve the detection of a threat, then any motion by the swarm prior to detection only uses energy unproductively. Therefore, we envision that in the detection stage, the swarm simply lies in wait, communicating infrequently, using as little energy as possible. When a contact is made, information is communicated to a neighborhood of gliders and the process of localization and confirmation begins.

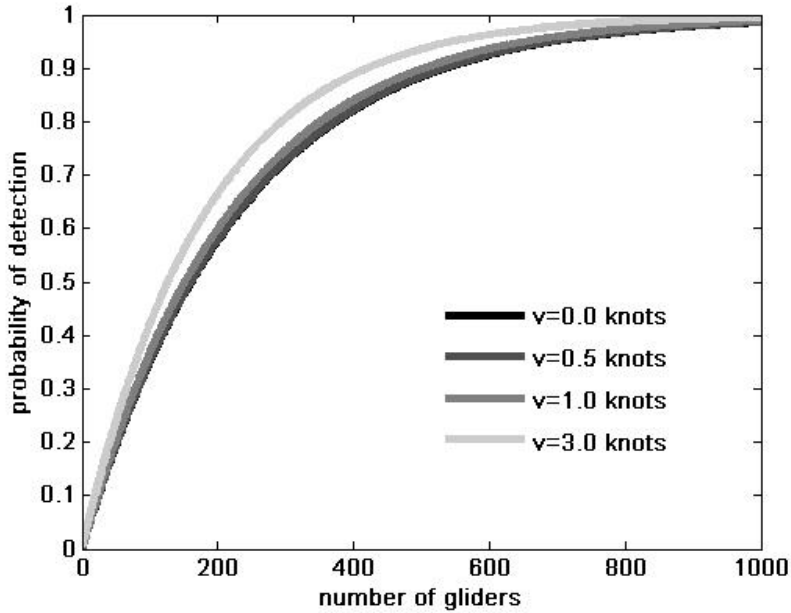


Figure 2: The probability of at least one detection by a swarm of gliders with various glider speeds. Notice that there is little change in the probability of detection with speed.

In the above section, we determined the probability of detecting a threat using derivations from Koopman. Results from this analysis showed that motion during the detection phase does little to improve the probability of detection. Nevertheless, as will be seen, motion significantly improves the ability for a swarm to localize, confirm or kill a threat. In section IV, we will derive the probability of a swarm of gliders confirming or killing a threat by expanding upon (1); however, to do so, we will need to use a modified derivation of this equation based upon disjoint events.

If $v = 0$, then from equation (1),

$$P_{g1}(S_d) = \frac{2RuT}{A} \quad (5)$$

where $2RuT$ is the area of the shaded rectangle in Figure 1. Noticing that the probability of detecting the threat in the time range $[t, t + dt]$ is given by

$$dP_{g1}(S_d, [t, t + dt]) = \frac{2Rudt}{A} \quad (6)$$

and that this is disjoint from the probability of detecting the threat within any other time range of length dt . Thus, we can rewrite equation (1) as

$$P_{g1}(S_d) = \int_0^T dP_{g1}(D, [t, t + dt]) . \quad (7)$$

Substituting (6) into (7) gives (5). Equation (6) and (7) will be revisited in section IV.

III. LOCALIZATION

As stated above, motion does little to improve the detection capability of the swarm. Nevertheless, once a contact is made, motion significantly improves localization, confirmation and kill.

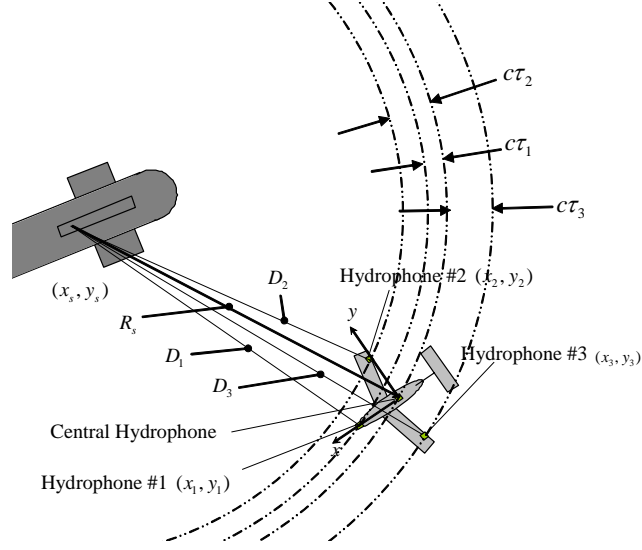


Figure 3: A glider and its hydrophones. Acoustic energy from a threat reaches the hydrophones at different times. The difference in these arrival times can be used to determine range and bearing.

Any model that is used to predict the effect of motion on the ability of a swarm to localize, confirm, and kill a threat must include a representation of measurement noise. In the following, we present one method of estimating the location of a threat from a set of sensors on the glider by measuring time delays between sensors. We then show how errors in these time delays translate to a positioning error relative to the coordinate system of the glider. This positioning error can then be translated into a global positioning error that can be used to drive an information filter. Information filters are used to estimate the location and speed of the threat in the presence of measurement noise.

a Measurement noise

A swarm of gliders attempts to discern a contact in the presence of noise. If it were not for noise, the process of confirming and localizing a threat would be trivial. Therefore, in any system level study, noise must be included. We assume that a glider contains a set of three hydrophones located about a central hydrophone (see Figure 3). Acoustic energy from a contact reaches these hydrophones at different times. The difference in arrival times between the central hydrophone and the i^{th} hydrophone is given by τ_i . Following the work of Huang, Benesty and Elko [5], these time differences can be used to estimate the location of a contact. A local coordinate system is defined with its origin at the central hydrophone and with the x axis along the length of the glider. Relative to this system, the vector between the central hydrophone and the i^{th} hydrophone is given by $\vec{r}_i = (x_i, y_i)$ where $|\vec{r}_i| = R_i$ is distance. The distance from the contact to the i^{th} hydrophone is given by D_i , and the distance from the contact to the central hydrophone is given by $|\vec{r}_s| = R_s$ where $\vec{r}_s = (x_s, y_s)$. From Huang, Benesty and Elko,

$$A\vec{\theta} = \vec{b} \quad (8)$$

where $A = \begin{bmatrix} x_1 & y_1 & c\tau_1 \\ x_2 & y_2 & c\tau_2 \\ x_3 & y_3 & c\tau_3 \end{bmatrix}$, $\bar{b} = \frac{1}{2} \begin{bmatrix} R_1^2 - (c\tau_1)^2 \\ R_2^2 - (c\tau_2)^2 \\ R_3^2 - (c\tau_3)^2 \end{bmatrix}$, and $\bar{\theta}^T = [\hat{x}_s, \hat{y}_s, R_s]^T$ is the measurement of

the location and distance of the contact relative to the local coordinate system of the glider. For contacts at the edge of the detection range, these measurements are highly corrupted by noise. Assuming that time delay estimates, τ_i , are uncorrelated and that all statistics are Gaussian, the variance of these measurements can be approximated as

$$\sigma^2 = E\left([\bar{\theta}' - E(\bar{\theta}')][\bar{\theta}' - E(\bar{\theta}')]^T\right) = \mathbf{T} \left(\sum_{i=1}^3 \frac{\partial A^{-1} \bar{b}}{\partial (c\tau_i)} \sigma_i^2 \left[\frac{\partial A^{-1} \bar{b}}{\partial (c\tau_i)} \right]^T \right) \mathbf{T}^T \quad (9)$$

where $\bar{\theta}'^T = [\hat{x}_s, \hat{y}_s]^T$, $\mathbf{T} = \begin{bmatrix} 1 & 0 & 0 \\ 0 & 1 & 0 \end{bmatrix}$, and $\sigma_i^2 = E([\tau_i - E(\tau_i)]^2)$.

If measurements are ergodic, τ_i can be estimated using the process shown in Figure 4 where σ_{τ_i} is the variance of τ_i . Pressure time histories are measured at the i^{th} and central hydrophones, band passed filtered between frequencies f_1 and f_2 , summed and integrated over time. Quazi [7] shows that if the signal to noise ratio, SNR , between f_1 and f_2 is constant, and $SNR \ll 1$ then

$$\sigma_{\tau_i} \approx \frac{1}{2\pi} \frac{1}{\sqrt{2T_{\text{int}}W}} \frac{1}{f_{\text{rms}}} \frac{1}{SNR} \quad (10)$$

where $W \equiv f_2 - f_1$, $f_{\text{rms}} = f_o \sqrt{1 + (W^2 / 12f_o^2)}$ and $f_o \equiv f_1 + W/2 = f_2 - W/2$. For $SNR \gg 1$

$$\sigma_{\tau_i} \approx \frac{1}{2\pi} \frac{1}{\sqrt{T_{\text{int}}W}} \frac{1}{f_{\text{rms}}} \frac{1}{\sqrt{SNR}}. \quad (11)$$

As the threat moves closer to the glider, SNR increases and σ_{τ_i} becomes small. As it moves farther away, the opposite occurs. Assuming that variations in SNR are dominated by two dimensional acoustic spreading, if d is the distance between the glider and the contact and SNR_R is the signal to noise ratio at detection range, R , then

$$SNR \approx SNR_R \cdot \frac{d}{R}. \quad (12)$$

where SNR_R and R are determined from the sonar equation (see Appendix I).

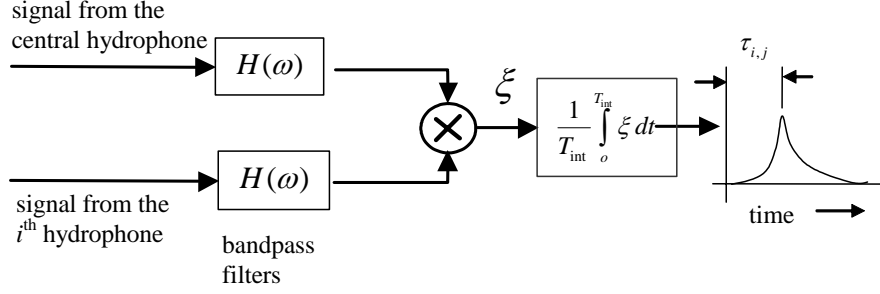


Figure 4: Time delays between hydrophones are measured using a cross correlation.

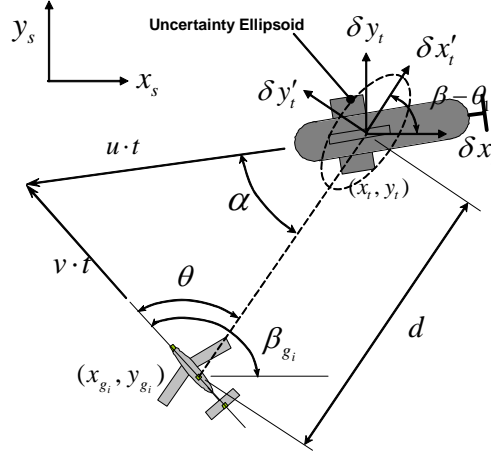


Figure 5. Range and bearing error can be translated into a local error in a coordinate system centered at the location of the threat. This error can be translated into global coordinates.

From the above equations a statistical estimate of the location of the threat relative to the local coordinate system of the glider can be made. Knowing the orientation and location of its own local coordinate system, a glider can translate these measurements into global coordinates (see Figure 5). If (x_t, y_t) is the true location of the contact in glider coordinates and $\delta x'_t = \hat{x}_s - x_t$ and $\delta y'_t = \hat{y}_s - y_t$ are the deviations of glider measurements from their true values in this same coordinate system, then the deviation of these measurements in global coordinates is given by

$$\vec{v} = \begin{bmatrix} \delta x_t \\ \delta y_t \end{bmatrix} = G \begin{bmatrix} \delta x'_t \\ \delta y'_t \end{bmatrix} \quad (13)$$

where $G = \begin{bmatrix} \sin(\beta - \theta) & -\cos(\beta - \theta) \\ \cos(\beta - \theta) & \sin(\beta - \theta) \end{bmatrix}$. Thus, assuming white noise, a sampled correlation matrix for measurement noise in global coordinates is given by

$$R = E(\vec{v}(i)\vec{v}^T(i-j)) = G\sigma G^T \delta_{ij} \quad (14)$$

where δ_{ij} is a Kronecker delta function, \vec{v} is measurement noise, and σ is defined in (9). In the following, we will use this measurement noise as input to an information filter for the purpose of

localizing a contact. This localization process occurs in a global coordinate system utilized by all gliders.

b Information filtering

Information filters [8] are used to share state predictions and to temporally minimize measurement noise. These filters, running in parallel, produce the same results as if measurements from all gliders were combined into a single Kalman [9] filter or as if identical Kalman filters were run in parallel and then fused [10]. Nevertheless, in general, the computational cost of using a Kalman filter is greater than that of using an information filter when several measurements are being processed at that same time and therefore, information filtering is presented here.

The information filter like the Kalman filter uses a mathematical model of the dynamics of a contact to estimate its state. This state can be used to determine the location and bearing of a contact. We assume that the contact has discrete-time dynamics that can be fit to the model

$$\bar{x}(k) = F \bar{x}(k-1) + \bar{w}(k-1) \quad (15)$$

$$\bar{z}(k) = H \bar{x}(k) + \bar{v}(k) \quad (16)$$

where $\bar{x}(k) = [x_t, y_t, u_{x_t}, u_{y_t}]^T$, (x_t, y_t) is the global location of the contact, $u_{x_t} = u \cos \beta_t$ is the velocity of the contact along the x axis, $u_{y_t} = u \sin \beta_t$ is the velocity of the contact along the y axis,

$$F = \begin{bmatrix} 1 & 0 & \Delta T & 0 \\ 0 & 1 & 0 & \Delta T \\ 0 & 0 & 1 & 0 \\ 0 & 0 & 0 & 1 \end{bmatrix}, \quad (17)$$

$$H = \begin{bmatrix} 1 & 0 & 0 & 0 \\ 0 & 1 & 0 & 0 \end{bmatrix}, \quad (18)$$

$\bar{w}(k) \in \mathfrak{R}^{4 \times 1}$ is the state noise with covariance $Q \in \mathfrak{R}^{4 \times 4}$, $\bar{z}(k) \in \mathfrak{R}^{2 \times 1}$ is the sensor measurement, and $\bar{v}(k) \in \mathfrak{R}^{2 \times 1}$ is the measurement noise with statistics as defined in (14). The state noise, $\bar{w}(k)$, is due to forces on the threat that produce a change of its position with time whereas the noise $\bar{v}(k)$ represents noise introduced into measurements as described above. Considering the size and mass of a threat, we assume that $\bar{w}(k)$ is insignificant compared to $\bar{v}(k)$. Therefore, we set $Q = c_0 I$ where $c_0 \approx 0$ is a small number and I is the identity matrix.

The information filter for the i^{th} glider consists of a prediction and estimation step. The local prediction step is

$$\hat{\bar{y}}_i(k|k-1) = Y_i(k|k-1) F Y_i^{-1}(k-1|k-1) \hat{\bar{y}}_i(k-1|k-1) \quad (19)$$

$$Y_i(k|k-1) = \left[F Y_i^{-1}(k-1|k-1) F^T + Q \right]^{-1} \quad (20)$$

where $\hat{y}_i(k|k-1)$ is the prediction of the information vector, $Y_i(k|k-1)$ is the prediction of the information matrix, $\hat{y}_i(k-1|k-1)$ is the previous estimate of the information vector, and $Y_i(k-1|k-1)$ is the previous estimate of the information matrix. The information vector and matrix are related to the state vector and its covariance by

$$E(\bar{x}(k)) = \hat{\bar{x}}(k) = Y_i^{-1}(k|k) \hat{y}_i(k|k) \quad (21)$$

$$E((\bar{x}(k) - E(\bar{x}(k)))(\bar{x}(k) - E(\bar{x}(k)))^T) = P(k) = Y_i^{-1}(k|k) \quad (22)$$

where $\hat{\bar{x}}(k) = [\hat{x}_i, \hat{y}_i, \hat{u}_{x_i}, \hat{u}_{y_i}]^T$ and \hat{x}_i is the estimate of x_i .

The estimation step is

$$\hat{y}_i(k|k) = \hat{y}_i(k|k-1) + \sum_{j \in NN} H^T R_j^{-1}(k) \bar{z}_j(k) \quad (23)$$

$$Y_i(k|k) = Y_i(k|k-1) + \sum_{j \in NN} H^T R_j^{-1}(k) H_j \quad (24)$$

where NN refers to the set of nearest neighbor gliders that have detected the threat at time step k and can communicate with the i^{th} glider.

Using equation (8) through (24), MATLAB, simulations of a threat moving past a stationary glider were produced (see Appendix II for parameters). Figure 6 shows the measurement and estimate of the x location of the threat (in global coordinates) by the glider. Notice that initially measurement error is very large; however as the threat moves past the glider, the range to the glider is reduced and SNR is enhanced. The estimate from the information filter improves, but with less variation. As the threat passes and the distance between the threat and the glider increases, SNR is reduced and variations in the measurement increase. Nevertheless, variations in the estimate are still small.

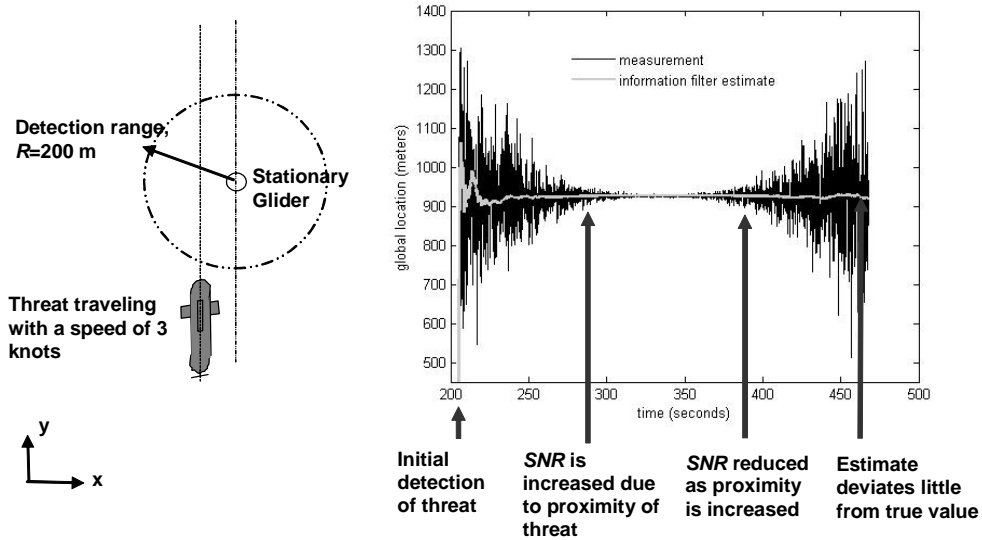


Figure 6: Measurement and prediction of the x location of threat. black – measurement, grey – estimate.

IV. CONFIRMATION AND KILL

As stated above, an information filter is simply a Kalman filter solved in a computationally efficient fashion and a Kalman filter is a dynamic filter used to reduce measurement noise based upon a model of threat dynamics. The result is a low noise estimate of the location of a contact. From this, a glider can estimate its ability to confirm or kill. Nevertheless, Kalman filtering is not perfect and due to the presence of residual noise, the probability of confirming or killing is probabilistic.

a A higher level of control

As shown in Figure 7, as a glider moves through the water, it asks itself a number of questions and based upon its response, it modifies its actions accordingly. This process begins with an interrupt that down-loads information about the location and type of a contact. The glider evaluates this data and acts upon its evaluation. For example, if the glider receives information that there is a confirmed threat, but deduces that it cannot kill this threat, there is no reason for it to move since additional motion will not add any information to the swarm. However, if it determines that it can kill the threat, it acts appropriately by moving. As the glider moves it evaluates the quality of its contact and whether or not it has the ability to kill. When it determines that it can no longer increase the level of information in the swarm, it breaks from pursuit and transfers any additional information to its neighbors. Other gliders receive this information and the process is begins again.

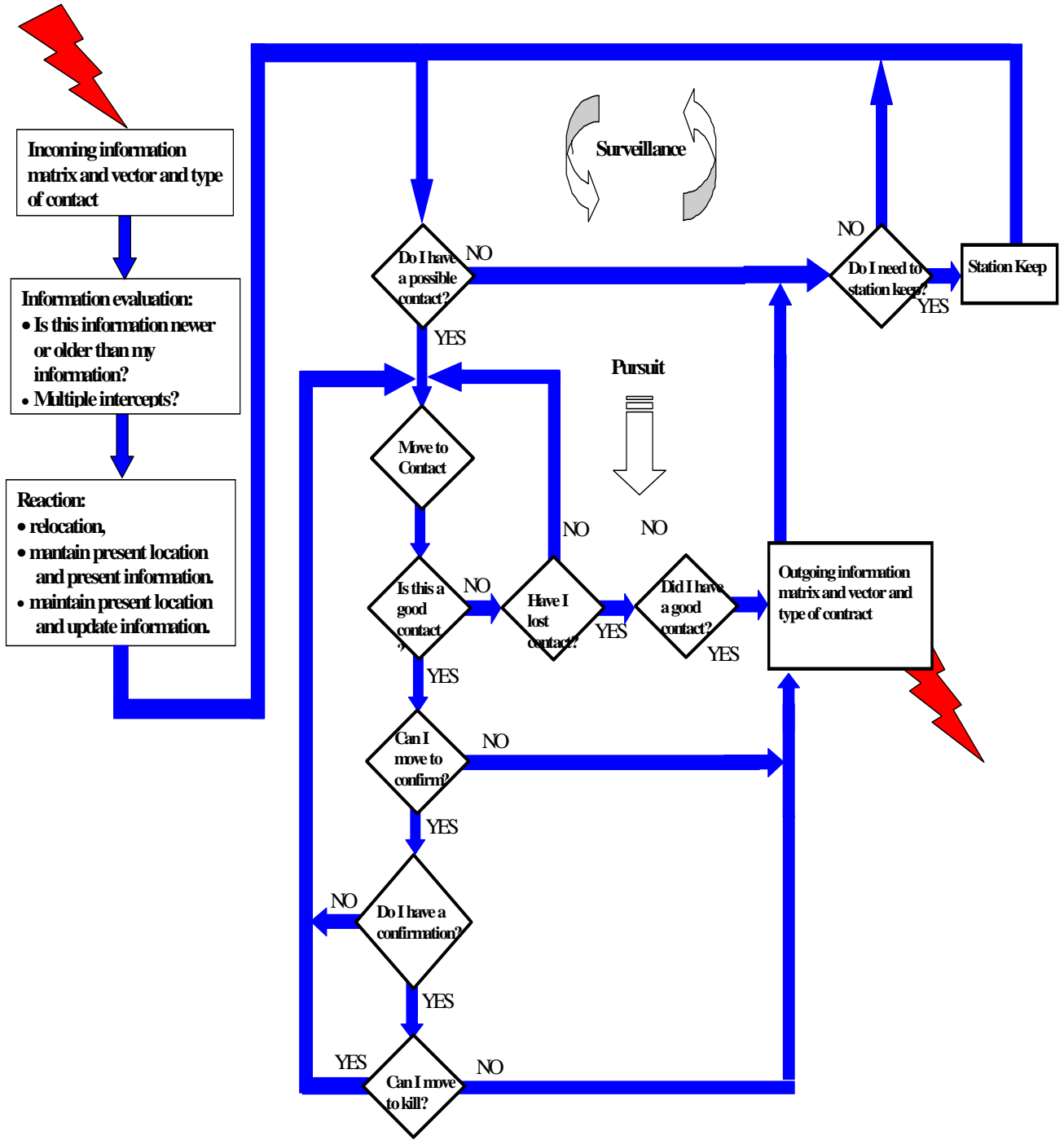


Figure 7: Upper layer of control based on a set of logic rules.

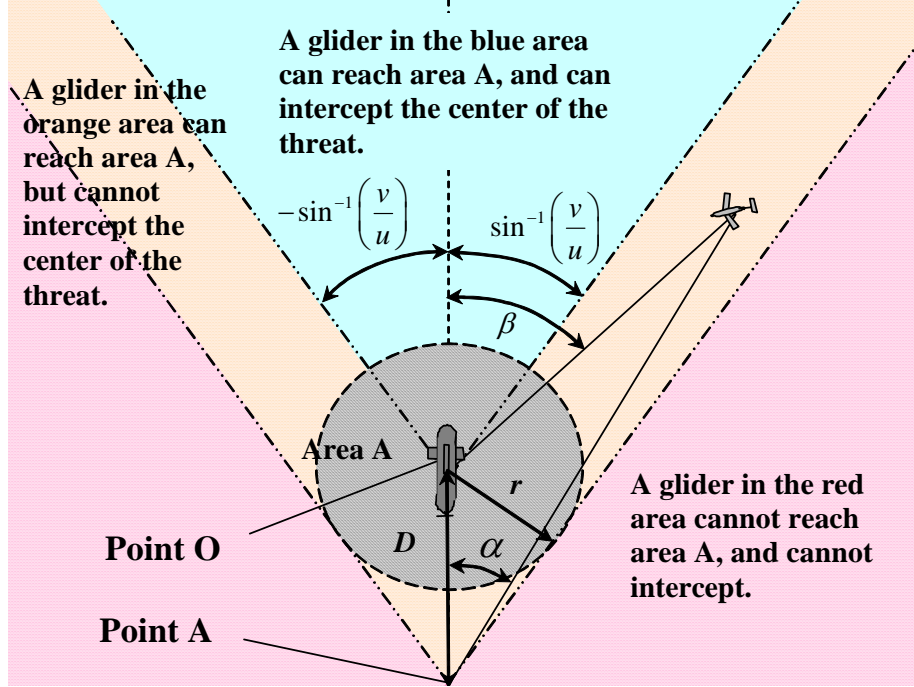


Figure 8: Region of approach to confirm and region of approach to kill.

The algorithm used to determine if a glider can confirm or kill a threat is an extension of the work of Koopman [1]. A glider can intercept the center of the threat if it lies within the region of approach. This region is defined by a cone extending from the threat to areas with an arch from $-\sin^{-1}\left(\frac{v}{u}\right)$ to $\sin^{-1}\left(\frac{v}{u}\right)$ from its direction of motion as shown in **Figure 8**. The apex of this cone is at the center of the threat. The region of approach to confirm or kill is given by the union of the orange and the blue areas in **Figure 8** and includes a cone between $-\sin^{-1}\left(\frac{v}{u}\right)$ to $\sin^{-1}\left(\frac{v}{u}\right)$ with apex at Point A at a distance D behind the location of the threat where

$$D = \frac{u}{v} r. \quad (25)$$

and $r = 30$ meters for confirmation and $r = 5$ meters to kill.

b A lower level of control

Figure 5 shows the location of the threat relative to the glider after detection. The shortest time to intercept can be calculated to be

$$\hat{t} = \frac{\hat{d}}{\hat{u}^2 - v^2} (\hat{u} \cdot \cos(\hat{\alpha}) - \sqrt{v^2 - \hat{u}^2 \cdot \sin^2(\hat{\alpha})}) \quad (26)$$

where \hat{d} is the distance between the glider and the contact, $\hat{u} = \sqrt{\hat{u}_x^2 + \hat{u}_y^2}$ is the speed of the threat, v is the speed of the glider, $\hat{\alpha}$ is calculated from threat bearing and location and variables with hats represent estimates from the information filter. From this equation comes the condition that the glider will intercept the target only if

$$\hat{\alpha} < \sin^{-1}\left(\frac{v}{\hat{u}}\right). \quad (27)$$

If this condition is satisfied, the glider must move in the direction

$$\theta = \sin^{-1}\left(\frac{\hat{u}}{v}\sin(\hat{\alpha})\right) \quad (28)$$

to intercept the threat in the shortest time. Equations (28) represent a simple control law for directing a glider to a threat with limited knowledge of threat dynamics.

c Swarm performance

A glider that makes contact can confirm or kill that contact one of two ways – it can confirm or kill it without help from any other glider, or it can confirm or kill by communicating with the other gliders and allowing another glider to do the confirming or killing for it. In this section we develop the probability of a glider confirming or killing without and with the aid of the rest of the gliders, combine these to determine the probability of a glider of confirming or killing, and then use this result to deduce the probability of the swarm confirming or killing. In the derivation below, we assume that the range of communication of each glider is enough that every glider can communication with any other glider in the 50x50 nautical mile box. We also assume that the gliders know their position, mostly likely via GPS.

Figure 9a shows the condition where the glider that detects the threat confirms or kills it. In this figure, a glider is a standoff distance χ away from a threat. As the threat passes, the glider detects it and moves to confirm and/or kill using the local control scheme given by equation (28), the information filter given by equations (15) through (24), and an approximation of noise given by equations (9) through (14). These simulations were run using the parameters given in Appendix II.

Monte Carlo simulations were run to determine the conditional probability of confirming or killing the threat as a function of χ given detection. Figure 9b shows these functions.

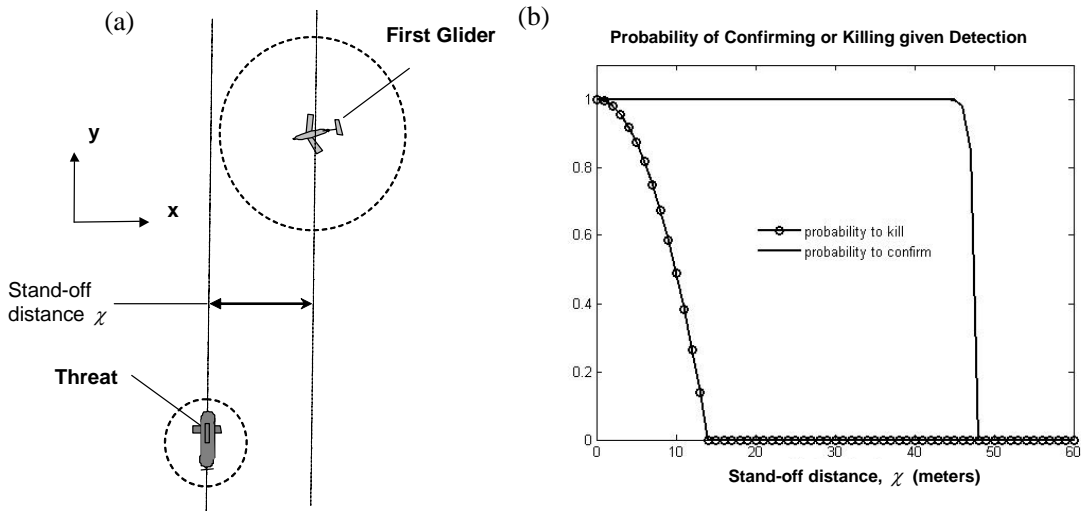


Figure 9: (a) Configuration used to run Monte Carlo simulations. (b) Results from Monte Carlo simulations.

The conditional probability functions in **Figure 9b** can be approximated by

$$f_{g1}(S_k | S_d) = \begin{cases} \frac{1}{200} \left(1 - \left(\frac{\chi}{14} \right)^2 \right) & \text{for } 0 < \chi < 14 \\ 0 & \text{for } 14 < \chi < 200 \end{cases}, \quad (29)$$

$$f_{g1}(S_c | S_d) = \begin{cases} \frac{1}{200} \left(1 - \left(\frac{\chi}{40} \right)^{90} \right) & \text{for } 0 < \chi < 40 \\ 0 & \text{for } 40 < \chi < 200 \end{cases} \quad (30)$$

where

$$S_k = \{ \text{the glider kills the threat} \}$$

$$S_c = \{ \text{the glider confirms the threat} \}.$$

From (29) and (30) the probability of killing and confirming the threat, given that the threat is detected is given by

$$P_{g1}(S_k | S_d) = \int_0^R f_{g1}(S_k | S_d) d\chi = 0.047, \quad (31)$$

$$P_{g1}(S_c | S_d) = \int_0^R f_{g1}(S_c | S_d) d\chi = 0.237, \quad (32)$$

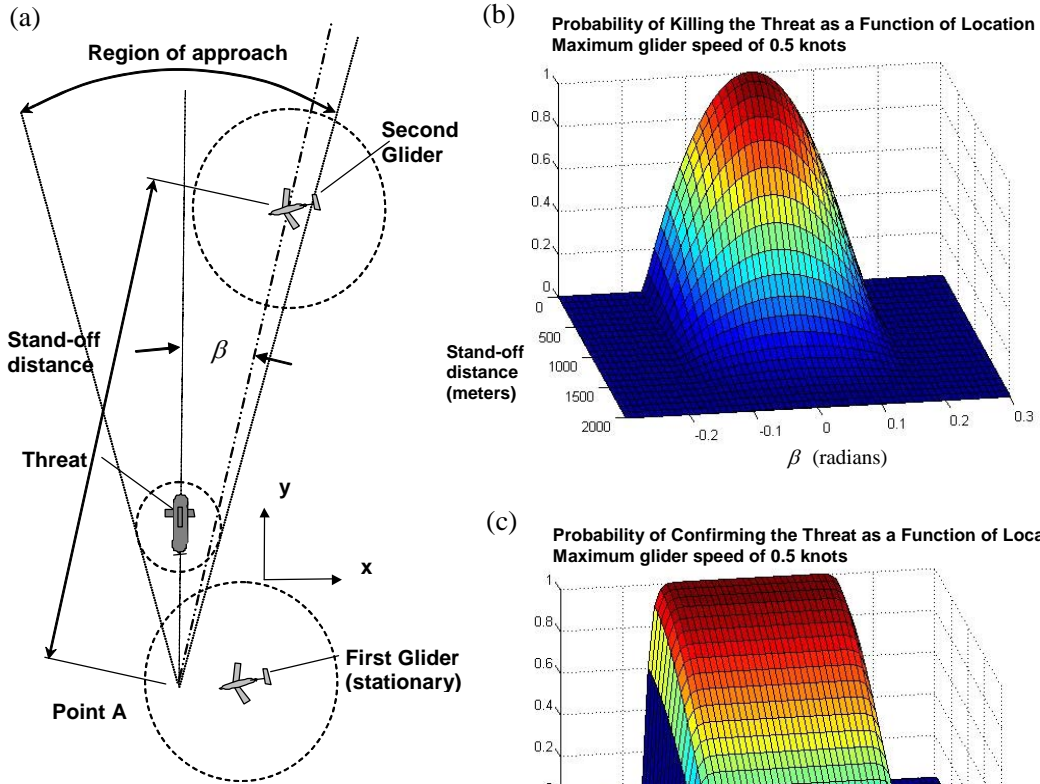
where R is detection range. In comparison, if the glider could not move,

$$P_{g1}(S_k | S_d) = \frac{r = 5 \text{ meters}}{r = 200 \text{ meters}} = 0.025 \quad \text{and} \quad P_{g1}(S_c | S_d) = \frac{r = 30 \text{ meters}}{r = 200 \text{ meters}} = 0.15$$

which are values significantly less than those given in (31) and (32). Thus, motion improves the ability of even a single glider to confirm and/or kill once detection occurs.

Figure 10 shows the condition where the glider that detects the threat communicates with the rest of the swarm so that another glider can confirm or kill. This figure is similar to the **Figure 9** system with a second glider in the region of approach at angle β and at a stand-off distance q . The first glider is assumed to be stationary. As the threat passes, the first glider transmits its information vector and matrix to the second glider. The second glider uses this information to attempt to confirm and/or kill.

Monte Carlo simulations were run to determine the probability of the second glider confirming and/or killing the threat given that detection occurred due to an initial glider located 75 meters in the x direction from threat. The probability of the second glider confirming or killing is plotted in **Figure 10b** and **c** as a function of position.



The first glider detects the threat and starts its information filter. It is assumed to be stationary. The threat moves as close as 75 meters from this glider and then moves outside its range of detection. The first glider transfers information filter data to the second glider and the second glider attempts to confirm or kill.

One hundred simulations were run for each point in a 7 by 61 grid of points in β and stand-off distance. Results were averaged and curved fit. The curve fitted results are shown in (a) and (b).

Figure 10: (a) Configuration used to run Monte Carlo simulation. (b) Probability of a kill. (c) probability of a confirmation.

From simulations, the below approximations can be made

$$P_{g_2}(S_k | (\beta, q)) = \begin{cases} \left\{ 1 - \left(\frac{\beta}{\beta_{\max}} \right)^\rho \right\} e^{-(\lambda \cdot (q-D))^2} & \text{for } -\beta_{\max} \leq \beta \leq \beta_{\max} \text{ and } D < \rho < \infty \\ 0 & \text{otherwise} \end{cases} \quad (33)$$

for $\rho = 2$ and $\lambda = 0.0018$ and

$$P_{g_2}(S_c | (\beta, q)) = \begin{cases} \left\{ 1 - \left(\frac{\beta}{\beta_{\max}} \right)^\rho \right\} e^{-(\lambda \cdot (q-D))^2} & \text{for } -\beta_{\max} \leq \beta \leq \beta_{\max} \text{ and } D < \rho < \infty \\ 0 & \text{otherwise} \end{cases} \quad (34)$$

for $\rho = 20$ and $\lambda = 0.0006$, where β is in radians and $\beta_{\max} = \sin^{-1} \frac{v}{u}$.

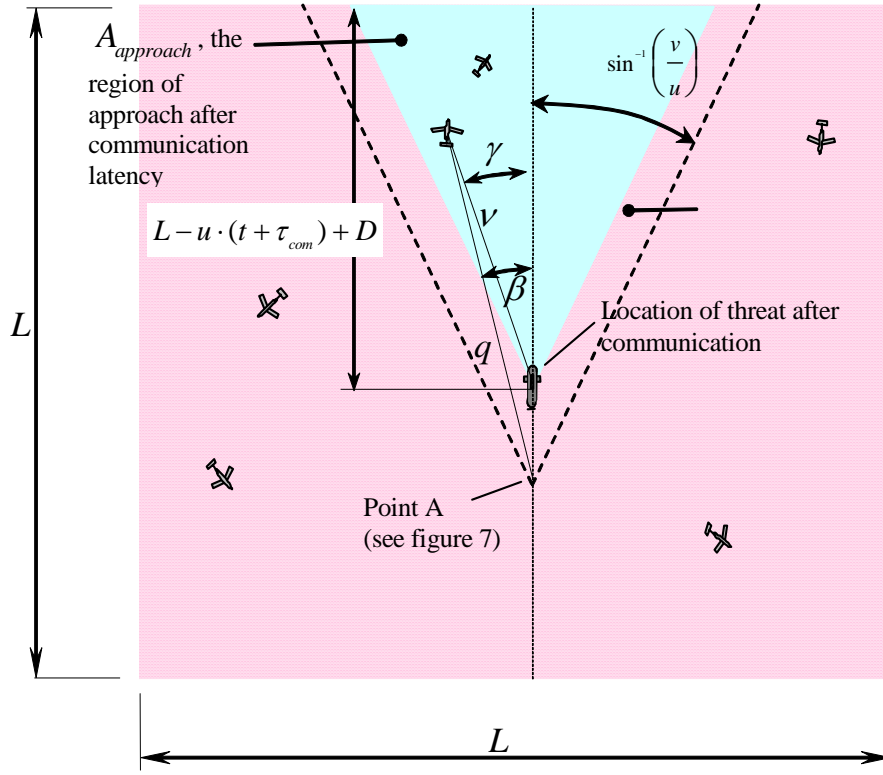


Figure 11: The region of approach is a function of confirmation and/or detection range and communication latency. The effect of a communications delay is to move the region of approach forward.

The probability of confirming a threat via communications to a second glider given detection within any time interval $[t, t + dt]$ by the first glider is a function of D (see equation (25)) and of the latency of communications, τ_{com} . An analysis of the latency of communications is given in Appendix III. As shown in Figure 11, the region of approach is bounded by the sea space shown in Figure 1. Assuming that the information statistics change little with the distance at which contact is made by the first glider, the probability of the second glider confirming a threat is given by

$$P_{g_2}(S_c | S_d, [t, t + dt]) = \frac{1}{A_{Approach}} \int P_{g_2}(S_c | (\beta, q)) \cdot v dv \cdot d\gamma. \quad (35)$$

where distance v and angle γ are as shown in Figure 11, $A_{approach}$ is that part of the region of approach within A with height $l = L - u \cdot (t + \tau_{com}) + D$

$$q = \sqrt{(v \cdot \cos \gamma + u \cdot \tau_{com})^2 + (v \cdot \sin \gamma)^2} \quad (36)$$

and

$$\beta = \cos^{-1} \left(\frac{v \cdot \cos \gamma + u \cdot \tau_{com}}{q} \right). \quad (37)$$

For the situation where β_{\max} is small (i.e. the gliders are much slower than the threat), using equation (34), equation (35) can be approximated by

$$P_{g_2}(S_c | S_d, [t, t + dt]) = \frac{\beta_{\max}}{A} \frac{\rho}{\rho + 1} \int_D e^{-\lambda^2(v + \tau_{com} \cdot u - D)^2} \cdot v dv. \quad (38)$$

Therefore, the probability that k secondary gliders will confirm the threat after communicating with the first glider is given by

$$P_N(S_c = k | S_d, [t, t + dt]) = \frac{n!}{k!(n-k)!} P_{g_2}(S_c | S_d, [t, t + dt])^k (1 - P_{g_2}(S_c | S_d, [t, t + dt]))^{n-k} \quad (39)$$

and therefore, the probability that at least one secondary glider will confirm the threat after communicating with the first glider is given by

$$P_N(S_c > 0 | S_d, [t, t + dt]) = 1 - P_N(S_c = 0 | S_d, [t, t + dt]). \quad (40)$$

Thus, using results from Section II, from (7), the probability of the first glider confirming a threat by communicating with the rest of the swarm is given by

$$P_{g_1}(S_{cN}) = \int_0^T P_N(S_c > 0 | S_d, [t, t + dt]) \cdot dP_{g_1}(S_d, [t, t + dt]) \quad (41)$$

where

$$S_{cN} = \{\text{a glider confirms the threat by communicating with other gliders}\}$$

and $dP_{g_1}(S_d, [t, t + dt])$ is defined by equation (6) in section II.

A similar solution can be derived for $P_{g_1}(S_{kN})$ where

$$S_{kN} = \{\text{a glider kills the threat by communicating with other gliders}\}.$$

Equation (32) is the probability of the first glider confirming the threat that it initially detected, and equation (41) is the probability of the first glider communicating with a second glider that confirms the threat given detection by the first glider. Thus, the probability that a single glider will confirm and/or kill the threat by communicating with the rest of the swarm or on its own is given by

$$P_{g_1}(S_c) = P_{g_1}(S_c | S_d) \cdot P_{g_1}(S_d) + (1 - P_{g_1}(S_c | S_d) \cdot P_{g_1}(S_d)) \cdot P_{g_1}(S_{cN}). \quad (42)$$

$$P_{g_1}(S_k) = P_{g_1}(S_k | S_d) \cdot P_{g_1}(S_d) + (1 - P_{g_1}(S_k | S_d) \cdot P_{g_1}(S_d)) \cdot P_{g_1}(S_{kN}) \quad (43)$$

where $P_{g_1}(S_d)$ is given by equation (5).

Thus, the probability that k gliders will confirm and/or kill the threat by communicating or on their own is given by

$$P_N(S_c = k) = \frac{n!}{k!(n-k)!} P_{g_1}(S_c)^k (1 - P_{g_1}(S_c))^{n-k}, \quad (44)$$

$$P_N(S_k = k) = \frac{n!}{k!(n-k)!} P_{g1}(S_k)^k (1 - P_{g1}(S_k))^{n-k}, \quad (45)$$

and the probability that at least one glider will confirm or kill the threat by communicating on its own is given by

$$P_N(S_{cN}) = 1 - P_N(S_c = 0), \quad (46)$$

$$P_N(S_{kN}) = 1 - P_N(S_k = 0). \quad (47)$$

Equations (46) and (47) represent the probability of a swarm of gliders to confirm or kill a threat. This probability can be compared to the probability of a distribution of stationary sensors confirming or killing the threat. For a non moving set of sensors, equations (3) through (5) are used with $r=30$ meters, the confirmation range. For the limiting case when glider speed is great than the speed of the threat confirmation and kill occurs for any detection. This can be represented by using equations (3) through (5) with $r=R$.

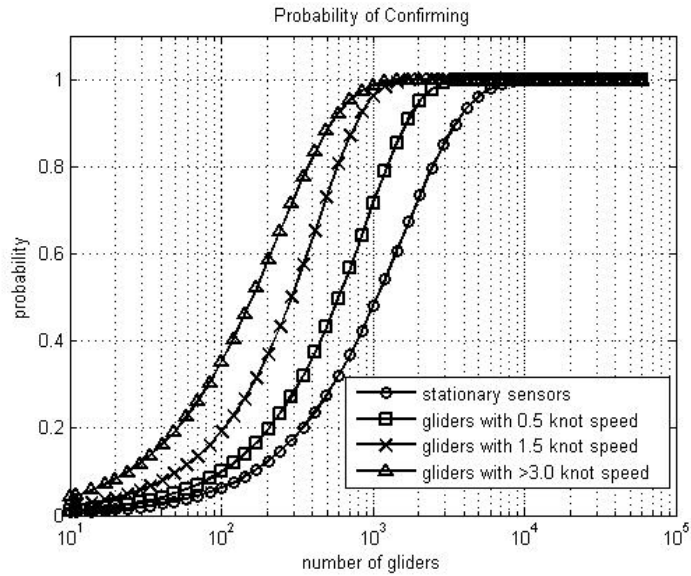


Figure 12: The probability of confirming a threat.

Figure 12 shows the probability of confirming a threat for a glider with speed 0.5 knots, 1.5 knot and any speed greater than the speed of the threat (3.0 knots). Figure 13 shows the same information for killing the threat.

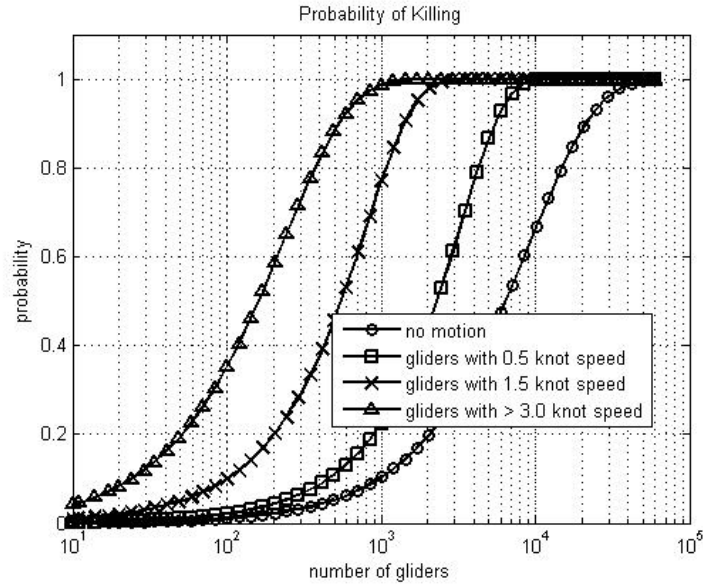


Figure 13: The probability of killing a threat.

Appendix III contains an analysis of communication latency. This is the time between when a glider detects a possible threat and the time this information is received by another glider. As discussed above this affects the probability of confirming or killing a threat; however, its affect is not as strong as might be expected. Figure 14 shows variations in the probability of confirming a threat as a function of communication latency. Notice that unless latency is on the order of hours, its effect is relatively weak. As pointed out in Appendix III, the typical latency to surface from a 200 meter depth will be less than 15 minutes. To maintain a probability of confirmation of 0.9, this 15 minute latency would reduce the performance of the swarm very little.

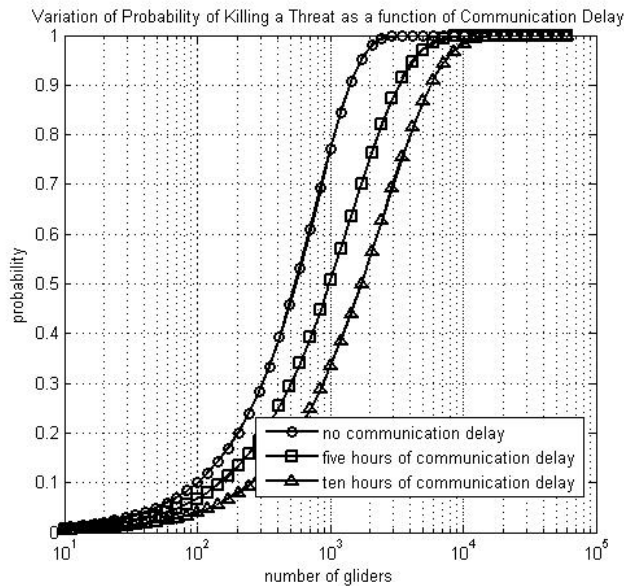


Figure 14: The variation in the probability of killing a threat as a function of communication delay. The glider has a speed of 1.5 knots.

If the width of the box shown in Figure 1 is reduced, the scenario approaches that of a barrier and the effects of time delay become more significant. Figure 15 shows the probability of confirming a

threat as a function of the number of gliders for a 1 hour communication delay and for various sea space widths. As the width of the sea space is reduced the number of glider required to produce the same probability of confirmation must increase since the size of the region of approach shown in Figure 11 (blue triangle) is reduced. When the width of the box is reduced to the point where the region of approach contains no area, the number of gliders must go to infinity. This occurs for the scenario in Figure 15 when the width is about 3.0 nm.

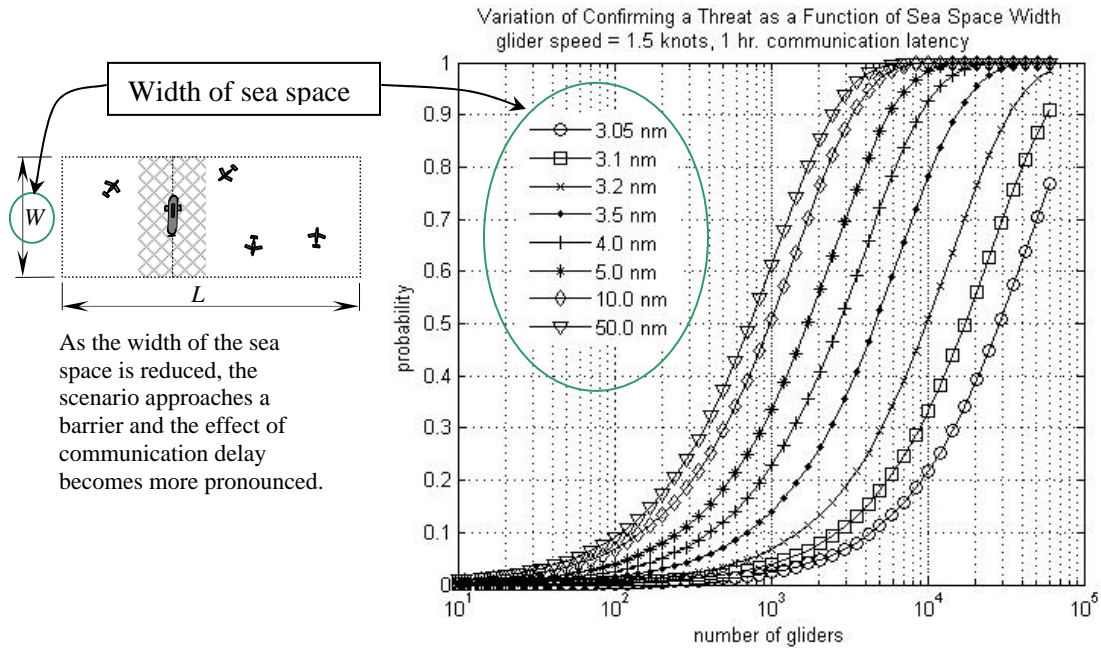


Figure 15: As the width of sea space is reduced, the affect of communication delay becomes more significant.

From Figure 12 and Figure 13 for glider speeds above the speed of the threat, the probability of confirming or killing the threat are the same. Therefore, to reduce the number of gliders needed to detect, confirm and kill a threat, the detection range needs to be increase. Figure 15 shows the probability of detecting, confirming and killing the threat as a function of range and number of gliders for a glider moving faster than the threat. Notice that to obtain a 90% probability of detecting, confirming and killing the threat using only 40 to 50 gliders, a 2400 meter range is required.

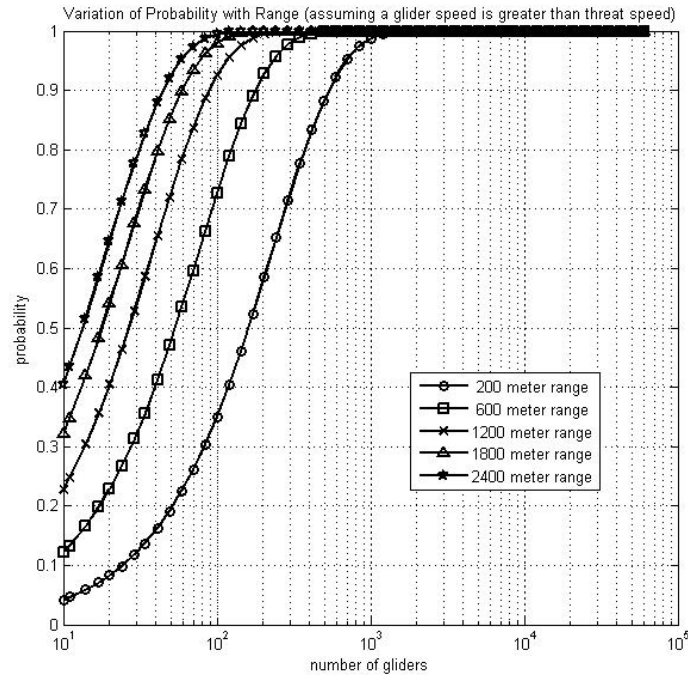


Figure 16: The probability of detecting, confirming and killing a threat as a function of range and number of gliders when the gliders can move faster than the threat.

V. CONCLUSIONS

From the above analysis, a number of conclusions can be drawn.

In Section II, it was determined that unless a glider can move much faster than the threat, the probability of initially detecting a threat is not a strong function of glider speed. Therefore, in the detection stage, it is best if gliders simply lie in wait for a threat. Once a threat is detected, information is passed to the rest of the swarm and gliders move to reduce their range for the purpose of confirming and/or killing the threat. Confirmation implies that the glider can move close enough to the threat that the threat can be characterized, and killing implies that the glider can intercept the threat.

Although motion does little to increase the probability of detecting the threat, it significantly improves the probability of confirmation and kill. Nevertheless, the range of improvement is bounded. Theory was developed to determine the effect of motion on confirming or killing a threat. This showed that as glider speed increases, this probability increases from the probability of a stationary sensor with detection range equal to the range required to confirm or kill to the probability of a stationary sensor where the range to confirm or kill has been equated to the detection range. Moreover, when the speed of the glider reaches the speed of the threat, the probability of detecting, confirming, and killing become equal. At this point, further enhancing the speed of the glider does little to improve its performance. To further improve performance or to reduce the number of gliders required, detection range must be increased. For example, in the case of acoustic detection with a range of 200 meters, it takes about 600 gliders to produce a 90% probability of detection, confirmation and kill. On the other hand, if the detection range were increased to 2400 meters, only 50 gliders would be required.

Communication latency was also studied. As is shown in Figure 14, communication latency on the order of one hour or less has a near negligible effect on performance when guarding a 50x50 nautical mile box. Therefore, methods of communication such as SATCOM, with longer latencies caused by the need to surface to communicate, will not significantly affect system performance.

VI. FUTURE WORK

Future work in the analysis of a swarm of glider should include reanalysis for a three dimensional problem, an analysis of the tradeoff between enhance detection range and energy consumption, a better understanding of how variations in glider distributions can affect swarm performance, an understanding of the effect of errors in glider location on swarm performance and an analysis of countermeasures against the swarm.

VII. REFERENCES

- [1] B.O. Koopman, Search and Screening, General Principles with Historical Applications, republished by the Military Operations Research Society, Alexandria, VA, 1999.
- [2] J.T. Feddema, "Sensor Networks for Collective Warfare," SAND2004-1578, Sandia National Laboratories Technical Report, May, 2004.
- [3] T.A. Wettergren, "Statistical Analysis of Detection Performance for Large Distributed Sensor Systems," NUWC-NPT Technical Report 11,436, June 2003.
- [4] S.L. Earp, *A Model for ASW Using Glider Fields*, report dated 11 March, 2004.
- [5] Y. Huang, J. Benesty, G. Elko, "Passive Acoustic Source Localization for Video Camera Steering," *IEEE Transactions on Acoustics, Speech, and Signal Processing*. Vol. ASSP-35, No. 8 August 1987.
- [6] A. Leon-Garcia, *Probability and Random Processes for Electrical Engineering, Second Edition*, Addison-Wesley, 1994.
- [7] A.H. Quazi, "An Overview on the Time Delay Estimate in Active and Passive Systems for Target Localization," *IEEE Transactions on Acoustics, Speech, and Signal Processing*, vol. Asp 29, No. 3, June 1981, pp. 527-533.
- [8] A.G.O. Mutambara, *Decentralized Estimation and Control for Multisensor Systems*, CRC, Boca Raton, 1998.
- [9] A. Gelb, *Applied Optimal Estimation*, the M.I.T. Press, Cambridge, MA.
- [10] S. Sun, "Multi-sensor optimal information fusion Kalman filters with applications," *Aerospace Science and Technology* 8 (2004) pp. 57-62.

APPENDIX I: DETECTION RANGE CALCULATION

Detection range is a key factor in determining the cost and capability of a sensor network. It is determined by the level of noise in the environment, the strength of the signal from the threat, the transmission of that signal through the water, and the ability for the detection system to enhance signal levels while rejecting noise. This can be summarized by the passive sonar equation¹

$$DT = SL - TL - NL + DI \quad (48)$$

where

DT is the Detection Threshold, the signal power across the bandwidth of detection normalized by the noise power in a one Hertz band;

NL is the background Noise Level of the ocean normalized by a reference pressure;

SL is the Source Level, the power of the signal emitted by the threat normalized to one yard from the geometric center of the threat and by a standard reference pressure;

TL is the Transmission Loss, the ratio of the received power of the signal at normalized by the power of the signal transmitted; and

DI is the Directivity Index, the ratio of the signal to noise of the array normalized by the signal to noise of a single element of that array.

Here we discuss each term on the right hand side of this equation for the purpose of determining *DT* as a function of distance from the threat.

Figure 17 is a copy of Wenz's illustration of noise in the oceans². Wenz not only shows noise from various sources but also shows the limits of prevailing noise. Below 1 kHz prevailing noise levels are substantial; however above 1 kHz, this noise is reduced and is a function of predominately surface wind speeds. For this reason, we limit our frequency range of interest to above 1 kHz. We also assume that the wind speeds of interested are below 20 knots, giving a maximum Beaufort number of 5 or a Sea State of about 4. We will also limit our maximum frequency of detection to below 10 kHz.

Urick combined Wenz's, Piggot's and Knudsen's data to produce Figure 18. Between 1 to 10 kHz, we can approximate *NL* by

$$NL = -15 \log(f) + 115 \text{ dB} . \quad (49)$$

Since the source levels of most threats are classified, we will use older data found in the open literature. Figure 19 shows the source level for a WWII fleet boat running a periscope depth. An approximation to this level in the frequency range of interest is given by

$$SL = -20 \log(f) + 176 \text{ dB} . \quad (50)$$

¹ R.J. Urick, *Principles of Underwater Sound/ 3d edition*, McGraw-Hill Book Company, New York, 1983.

² G.M. Wenz, "Acoustic Ambient Noise in the Ocean: Spectra and Sources," *Journal of the Acoustical Society of America*, vol. 34, no. 12, December 1962

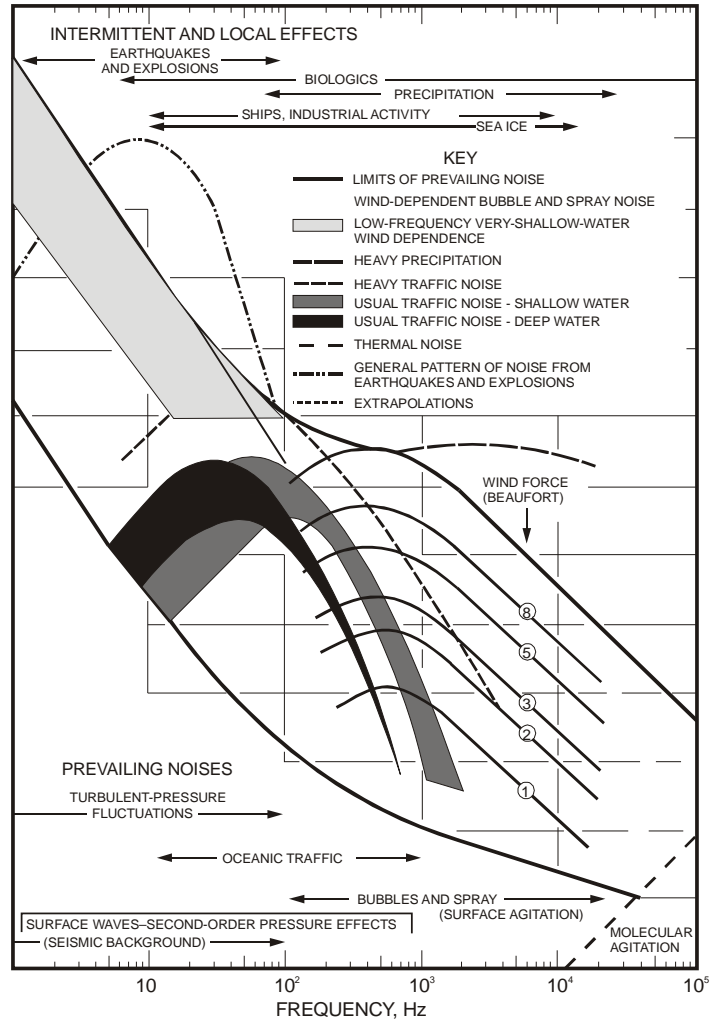


Figure 17: Wenz's illustration of back ground noise in the oceans: For frequencies above 1 kHz, noise level are low and are dominated by surface wind speed.

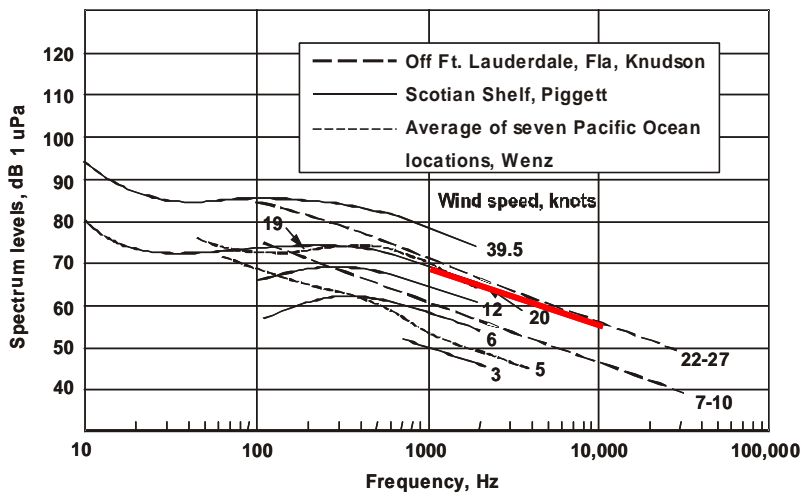


Figure 18: Urick's combination of data from Wenz, Piggot, and Knudsen: The red line shows the equation (49) approximation to NL for sea state 4 between 1 to 10 kHz.

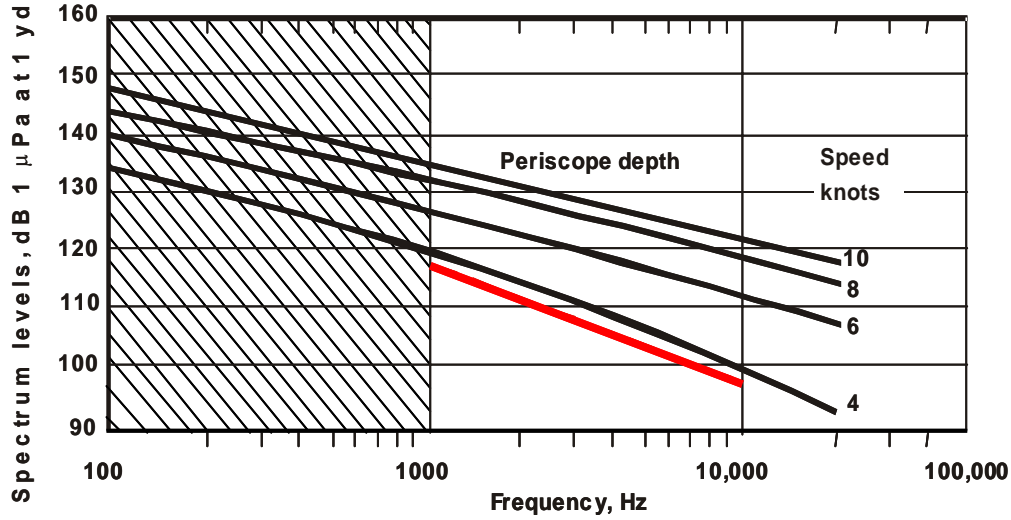


Figure 19: Spectrum of a WWII fleet boat running a periscope depth: The red line is the equation (50) approximation.

Transmission loss in the littoral can be found from the approximations of Marsh and Schulkin³. Marsh and Schulkin present the following three equations for the approximation of transmission loss at different distances, r , from the threat.

$$\text{For } r < H : TL = 20 \log_{10}(r) + \alpha r + 60 - k_L \quad (51)$$

$$\text{for } H \leq r \leq 8H : TL = 15 \log_{10}(r) + \alpha r + a_T \left(\frac{r}{H} - 1 \right) + 5 \log_{10} H + 60 - k_L \quad (52)$$

$$r > 8H : TL = 10 \log_{10}(r) + \alpha r + a_T \left(\frac{r}{H} - 1 \right) + 10 \log_{10} H + 64.5 - k_L \quad (53)$$

where $H = \left[\frac{1}{8}(D + L) \right]^{\frac{1}{2}}$, D is the depth of the littoral, L is the depth of any layer, α is the attenuation of the surrounding water in dB per kiloyards, and k_L and a_T are given in the following tables.

frequency (Hz)	k_L for a sand bottom	k_L for a mud bottom
1000	4.1	3.7
2000	3.5	3.1
4000	2.9	2.4
8000	2.3	1.9
10000	2.2	1.7

Table 1: Near- Field anomaly coefficients.

³ H.W. Marsh, M. Schulkin, "Shallow Water Transmission," *Journal of Acoustical Society of America*, vol. 34, pp. 863, 1962.

frequency (Hz)	a_T for a sand bottom	a_T for a mud bottom
1000	2.9	4.1
2000	3.5	5.0
4000	4.1	6.2
8000	5.0	7.3
10000	5.2	7.8

Table 2: Attenuation factors.

The value of α can be approximated between 1 to 10 kHz by

$$\alpha = \frac{0.1 \cdot \left(\frac{f}{1000}\right)^2}{1 + \left(\frac{f}{1000}\right)^2} + 0.008 \cdot \left(\frac{f}{1000}\right)^2 \quad (54)$$

where f is in Hertz.

The directivity index, DI, is the ratio of the signal to noise of an array of sensors to the signal to noise of a single element. Here, we assume the DI~5.

Using the above data, equation (48) can be solved for DT. Figure 20 shows the value of DT versus frequency for various ranges, R.

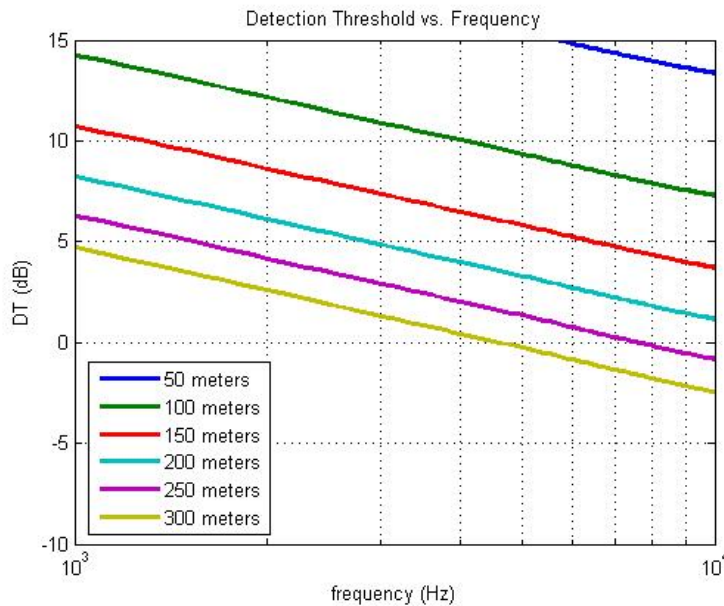


Figure 20: Detection Threshold as a function of frequency for various ranges from the threat:

We assume power law detection as shown below. Signal energy is band pass filtered, squared, and time integrated for time T . An optimal threshold is then watched to declare detection. Peterson,

Birdsall, and Fox⁴ relate the optimal parameters for this detection scenario to DT . For low signal to noise ratios

$$DT = 5 \log \frac{d\omega}{t} \quad (55)$$

where d is the detection index, ω is the bandwidth (in Hz), and t is the duration of the signal (here $t=T$). The detection index is obtained from the receiver operating characteristics curve (ROC). A ROC curve for Gaussian noise is shown in Figure 21. If we assume that a 1% probability of false alarm is acceptable for a 50% probability of detection, then $d=6$. Moreover, for a 200 meters detection range and a center frequency of 1 kHz, $DT=7$. Assuming a 100 Hz band pass filter, from equation (55), the integration time must be $t = T = 24$ seconds .

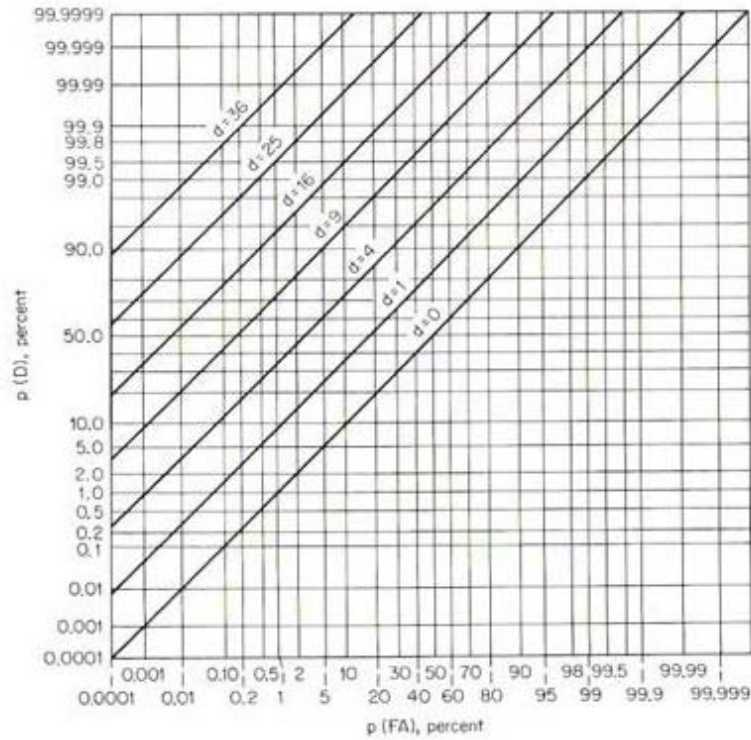


Figure 21: Receiver Operating Characteristics (ROC) for Gaussian noise.

⁴ W.W. Peterson, T.G. Birdsall, W.C. Fox, "The Theory of Signal Detectability," *Transactions of IRE*, PGIT-4, pp 171, 1954.

Intentionally Left Blank

APPENDIX II: SIMULATION PARAMETERS

The below table contains parameters used to produce Figure 6, Figure 9 and Figure 10.

Simulation Parameter	Description
$R= 200$ m	Detection range
$R_i = 1$ m	Distance between hydrophones on glider. With respect to the local coordinate system of the glider, hydrophones are located at $(x_1, y_1) = (1, 0)$ m, $(x_2, y_2) = (0, -1)$ m, and $(x_3, y_3) = (0, 1)$ m.
$c=1500$ m/s	Speed of sound in water
$T_{\text{int}} = 25$ seconds	Integration time used to calculate time delays.
$f_o = 500$ Hz	Center frequency used to calculate time delays.
$W= 1000$ Hz	Band width
$SNR_R = 7$	Signal to noise ratio at detection range
$\Delta T = 0.2$ s	Sampling time
$u = 3$ knots	Speed of threat
$v = 0.5$ knots	Speed of glider unless stated otherwise
$c_o = 1 \cdot 10^{-8}$	Coefficient used to define noise, w

Intentionally Left Blank

APPENDIX III: LATENCY OF COMMUNICATIONS

Satellite Communications, SATCOM:

There are a number of Low Earth Orbiting (LEO) systems than can be used for SATCOM communications; however, due to its ubiquitous presence and low orbital distance, the Iridium system is emphasized here. This system is nationally owned, containing 66 satellites at an altitude of 785 km. There is always an Iridium satellite at least within 8 degrees from the horizon at any location on the earth. The system uses the L band (1.6 GHz, 0.2 meter wavelength) for uploading and downloading data with bit rates up to 2.4 kbps. Only about 2 W of transmit power are required to reach an Iridium satellite.

Once a glider is on the surface, a SATCOM system can transmit information very quickly. Assuming a six by six information matrix and a six by one information vector comprised of 32 bit words about 1400 bits of information need to be communicated to update the location of a threat. This is the minimum amount of data to be transmitted not including bits for the preamble, message header, id number, time stamp and location. At 2 kbps this takes 0.7 seconds and at 2 watts of power, only 1.4 J of energy.

A limitation to the use of the Iridium system is its dying orbit.

Over-the-Horizon Radio Frequency, Communications:

Gliders can also communicate across the surface of the ocean; however, due to enhance path loss, the range to which they can transmit is limited compare to SATCOMs. To determine the range of communications, we use the equation

$$[P_r] = [P_t] + [G_t] + [G_r] - [P_L] \quad (56)$$

where $[P] = 10 \log_{10} P$, $[P_r]$ is received power (in dB referenced to milliwatt), $[P_t]$ is transmitted power, $[G_t]$ is transmitter antenna gain, $[G_r]$ is receiver antenna gain and $[P_L]$ is path loss. The path loss of an electromagnetic wave over a surface is significantly greater than that to a satellite. For transmission over a smooth surface

$$P_L = \left(\frac{d^2}{h_1 \cdot h_2} \right)^2 \quad (57)$$

where h_1 and h_2 are the heights of the receiver and transmitter antennas. Note, path loss varies with the fourth power of distance and as the height of an antenna goes to zero, this loss become infinite. These two effects, significantly limit the ability for communications to occur over the surface of the ocean. For $[P_r] = -95$ dBm, $[G_t] = 0$ dB, $[G_r] = 0$ dB, and $h_1 = h_2 = 2$ m, we can obtain an estimate of the range of an over-the-horizon RF communication system. Here, we also include an additional 10 dB increase in the path loss to account for the effects of a rough ocean. Figure 22 shows a plot of range versus transmitter power under these assumptions. Notice that 2 W will transmit up to 1 nm. This is much less than the 758 km (410 nm) range of a SATCOM system.

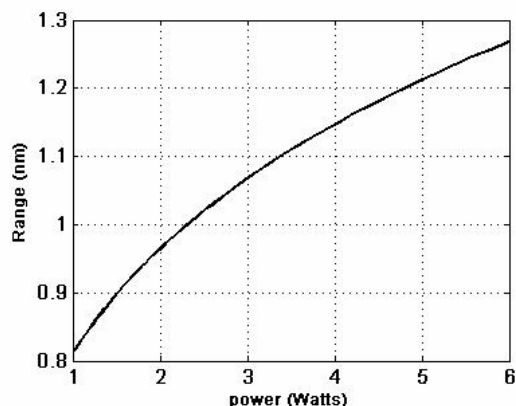


Figure 22: Communication range between gliders for a network of gliders using over the surface RF transmission.

Acoustic Communications, ACOMS:

Calculations similar to those made for SATCOM and RF could be made for ACOMS. However, the details of these calculations are more subjected to error due to the nature of the problem, therefore, we rely upon the work of Catipovic⁵ and Baggeroer⁶ as to the capability of such a system. From this work we can expect an ACOMS system operating in the littorals to have ranges up to 5 nm, sources transmitting on the order of 100 watts, frequencies between 10 to 100 kHz, and bit rates on the order of 100 bps. Notice that these powers and speeds are much higher and slower than those for a SATCOM or RF systems (requiring less than 10 watts of power and having bit rates on the order of 1 kbps). Nevertheless, just because they use less power to transmit and have faster bit rates does not imply they are better systems since RF and SATCOMS can only be used on the surface and energy must be expended to reach this position.

As stated above, we expect that over 1400 bits of data will need to be transmitted during each transmission⁷. Using an ACOMS system this will require about 15 seconds of transmit time and about 1400 J of energy. With an RF or SATCOM system this will require only 0.7 seconds of transmit time and about 1.4 J of energy. However, this is not all the energy or time that would be required to use RF or SATCOM since the glider must come to the surface in order to transmit. The difference between the above two energies is about 1398 J. Assuming that each system is allotted the same amount of energy to transmit a message, this would be the amount of energy available for the glider to reach the surface in the RF or SATCOM system. If one assumes an average glider depth of 100 m, then the average force required to bring a glider to the surface expending this excess amount of energy would be 14.0 N, and, assuming a drag coefficient of about 0.5 and a drag area of 1 sq. m, the average speed of this glider would be about

⁵ J.A. Catipovic, Performance Limitations in Underwater Acoustic Telemetry, IEEE Journal of Oceanic Engineering, vol. 15, no. 3, 1990.

⁶ A.B. Baggeroer, Acoustic Telemetry – An Overview, IEEE Journal of Ocean Engineering, vol. OE-9, no. 4, 1984.

⁷ From the August report this would include the information vector and matrix for a three dimensional problem and additional information on the character of the contact.

$$v = \sqrt{\frac{2 F_d}{\rho C_d A}} = \sqrt{\frac{2 \cdot 14.0}{1000 \cdot 0.5 \cdot 1}} = 0.24 \text{ m/s}.$$

At this speed, it will take 7 minutes for the glider to reach the surface – a time much longer than the transmit time for a single ACOMS transmission. Thus, on average, assuming equal amounts of energy for transmission, the time required to transmit an ACOMS signal is significantly less than that for a RF or SATCOM system.

Nevertheless, as was discussed in the text, even an hour latency delay does little to the performance of the swarm. A summary of communication benefits and limitations are given in the below table.

System	SATCOM 1.6 GHz (L band transmission), 100% coverage with ~ 2 W, kbps bit rates.	RF 900 MHz transmission frequencies. Low power ~ 2 W, kbps bit rates.	ACOMS 10 to 100 kHz transmission frequencies. 100 W or more power levels, 100's of bps bits rates.
Benefits:	<ul style="list-style-type: none"> ○ Ability to contact any surfaced glider and transmit out of network. ○ Ability to construct a central processing station to store data, process and transmit at a latter time. ○ Proven commercial system. 	<ul style="list-style-type: none"> ○ Limited to nearest neighborhood communications. 	<ul style="list-style-type: none"> ○ Limited to nearest neighborhood communications.
Limitations:	<ul style="list-style-type: none"> ○ Must surface to communicate requiring added power. ○ Not stealth. ○ Dying orbits limit the life of the system 	<ul style="list-style-type: none"> ○ Short ranges. ○ Must surface to communicate requiring added power. ○ Can only communicate with other gliders that are surfaced. 	<ul style="list-style-type: none"> ○ May not be stealth to the local threat. Communication range is much larger than detection range.
Latency	10s of minutes assuming the same amount of energy is used as in an ACOMS system. Less than a second assuming that the glider is already on the surface.	10s of minutes assuming the same amount of energy is used as in an ACOMS system. Less than a few seconds assuming that the glider is already on the surface.	○ 10s of seconds.

Table 3: Latency of communication.

DISTRIBUTION LIST

K. Latt
DARPA/ATO,
3701 North Fairfax Drive,
Arlington VA 22203-1714

searp@sle.vacoxmail.com S. Earp

D. Mihalak
1611 North Kent Street
Suite 700
Arlington, VA 22209

rtm@apl.washington.edu R. Miyamoto
jcl@apl.washington.edu J. Luby

G.McNamara
Manager Emerging Technologies
Naval Undersea Warfare Center
Newport, RI 02841-1708

MS 0617	J. Jakubczak, 12655
MS 0741	R. Robinett III, 6200
MS 0961	J. Harris, 14130
MS 1003	J. Feddema, 15211 (5)
MS 1002	P.Heermann, 15230
MS 1073	M. Daily, 1738
MS 1073	J. Dohner, 1738 (15)
MS 1221	G. Sanzero, 1316
MS 9018	Central Technical Files, 8945-1
MS 0899	Technical Library, 9616 (2)